Kinetic Modeling of β-Chloroprene Metabolism: I. *In vitro* Rates in Liver and Lung Tissue Fractions from Mice, Rats, Hamsters, and Humans

Matthew W. Himmelstein,[1] Steven C. Carpenter, and Paul M. Hinderliter

*E.I. du Pont de Nemours and Company, Haskell Laboratory for Health and Environmental Sciences,
PO Box 50, 1090 Elkton Road, Newark, Delaware 19711*

Beta-chloroprene (2-chloro-1,3-butadiene, CD) is carcinogenic by inhalation exposure to B6C3F1 mice and Fischer F344 rats but not to Wistar rats or Syrian hamsters. The initial step in metabolism is oxidation, forming a stable epoxide (1-chloroethenyl)oxirane (1-CEO), a genotoxicant that might be involved in rodent tumorigenicity. This study investigated the species-dependent *in vitro* kinetics of CD oxidation and subsequent 1-CEO metabolism by microsomal epoxide hydrolase and cytosolic glutathione *S*-transferases in liver and lung, tissues that are prone to tumor induction. Estimates for Vmax and Km for cytochrome P450-dependent oxidation of CD in liver microsomes ranged from 0.068 to 0.29 μmol/h/mg protein and 0.53 to 1.33 μM, respectively. Oxidation (Vmax/Km) of CD in liver was slightly faster in the mouse and hamster than in rats or humans. In lung microsomes, Vmax/Km was much greater for mice compared with the other species. The Vmax and Km estimates for microsomal epoxide hydrolase activity toward 1-CEO ranged from 0.11 to 3.66 μmol/h/mg protein and 20.9 to 187.6 μM, respectively, across tissues and species. Hydrolysis (Vmax/Km) of 1-CEO in liver and lung microsomes was faster for the human and hamster than for rat or mouse. The Vmax/Km in liver was 3 to 11 times greater than in lung. 1-CEO formation from CD was measured in liver microsomes and was estimated to be 2–5% of the total CD oxidation. Glutathione *S*-transferase-mediated metabolism of 1-CEO in cytosolic tissue fractions was described as a pseudo-second order reaction; rates were 0.0016–0.0068/h/mg cytosolic protein in liver and 0.00056–0.0022 h/mg in lung. The observed differences in metabolism are relevant to understanding species differences in sensitivity to CD-induced liver and lung tumorigenicity.

Key Words: 2-chloro-1,3-butadiene; microsomes; cytosol; liver; lung; mouse; rat; hamster; human; *in vitro* kinetics.

Beta-chloroprene (2-chloro-1,3-butadiene, CD, CAS 126-99-8) is a volatile colorless liquid used to manufacture polychloroprene, a synthetic rubber (Lynch, M. A., 2001). Occupational exposure occurs during monomer synthesis, shipping, and polymerization processes, and inhalation is the only significant route of exposure (Lynch, J., 2001). Cancer epidemiology studies have been inconclusive (Acquavella and Leonard, 2001; Colonna and Laydevant, 2001; Zaridze *et al.*, 2001).

The need to understand possible adverse health effects in humans has led to extensive evaluation of CD in experimental animals. Recent literature reviews have described the acute, subchronic, and chronic toxicity (Melnick and Sills, 2001; Valentine and Himmelstein, 2001). The most significant finding was CD-induced tumorigenicity in F344/N rats and B6C3F1 mice exposed to ≤80 ppm for 2 years (Melnick *et al.*, 1999, 1996; NTP 1998). Tumors in Fischer rats included the lung, oral cavity, thyroid gland, kidney, and mammary gland. Mouse tumors were observed in the lung, circulatory system, Harderian gland, forestomach, kidney, mammary gland, skin, mesentery, Zymbal gland, and liver. In contrast, no tumors were observed in Syrian hamsters. A weak response in mammary tissue was observed in female Wistar rats exposed to 10 or 50 ppm CD for up to 2 years (Trochimowicz *et al.*, 1998).

In vitro genotoxicity studies revealed that CD is mutagenic, primarily in bacterial reverse mutation assays with metabolic activation, while other *in vitro* and *in vivo* assays for either gene mutation or structural chromosomal damage were negative (Drevon and Kuroki, 1979; Foureman *et al.*, 1994; NTP, 1998; Tice, 1988; Tice *et al.*, 1988; Vogel, 1979). A recent study showed that a known CD metabolite, racemic (1-chloroethenyl)oxirane (1-CEO), was mutagenic in three *Salmonella typhimurium* strains (Himmelstein *et al.*, 2001b).

The *in vitro* biotransformation of CD has been studied to identify metabolites that might contribute to toxicity or mutagenicity (Bartsch *et al.*, 1979). More recently, the microsomal metabolism of CD to 1-CEO was confirmed as a cytochrome P450-dependent reaction (Himmelstein *et al.*, 2001a), and the S- and R-enantiomers of 1-CEO were identified (Cottrell *et al.*, 2001). Enzyme-mediated hydrolysis of 1-CEO occurred by microsomal epoxide hydrolase (Cottrell *et al.*, 2001; Himmelstein *et al.*, 2001a). Conjugation of 1-CEO with GSH has been shown in liver cytosolic fractions (Himmelstein *et al.*, 2001a), consistent with earlier *in vivo* studies showing depletion of

[1] To whom correspondence should be addressed. Fax: (302) 366-5003. E-mail: matthew.w.himmelstein@usa.dupont.com.

18

nonprotein sulfhydryls and the presence of thioethers in urine of rodents exposed to CD (Jaeger *et al.*, 1975; Plugge and Jaeger, 1979; Summer and Greim, 1980).

The goal of this research was to quantify the *in vitro* rates of CD-related biotransformation reactions in liver and lung tissue fractions of the rodent strains tested in the cancer bioassays and humans. Liver and lung were studied, because these tissues were prone to tumor induction and represented tissues important to xenobiotic metabolism. The simultaneous time course of cytochrome P450-dependent oxidation of CD was compared with rates of 1-CEO formation and hydrolysis, using a two-compartment kinetic model to account for the volatility of both analytes.

MATERIALS AND METHODS

Chemicals. β-Chloroprene (>99%) containing phenothiazine and N-nitrosodiphenylamine inhibitors was supplied by DuPont-Dow Elastomers LLC (LaPlace, LA). The inhibitors were removed as previously described (Himmelstein *et al.*, 2001a). The synthesis of (1-chloroethenyl)oxirane (1-CEO, >98%) was previously described (Himmelstein *et al.*, 2001a). Both the CD and 1-CEO were stored under nitrogen headspace at <-70°C and −20°C, respectively. Other chemicals used were of the highest purity available.

Source of microsomes and cytosol. Rodent liver microsomes and cytosol were purchased from two suppliers (*In Vitro* Technologies, Baltimore, MD or XenoTech, Lenexa, KS). Both suppliers used differential centrifugation as the method of preparation. Microsomes and cytosol were prepared from pooled livers from male B6C3F1 mice, Fischer F344 rats, Wistar rats, or Golden Syrian hamsters obtained from Charles River Laboratories (Raleigh, NC). Rodent lung microsomes and cytosol were prepared in-house using animals obtained from Charles River Laboratories. The fractions were prepared by differential centrifugation as previously described (Csanády *et al.*, 1992; Guengerich, 1994). All fractions were stored at <-70°C.

Human tissue fractions were also prepared by differential centrifugation. For experiments involving hydrolysis of 1-CEO, pooled liver microsomes from 15 individuals were used (Lot #1032, *In Vitro* Technologies). Experiments involving simultaneous CD and 1-CEO measurements used pooled liver microsomes from 10 individuals (Lot# 0010186, H1000, XenoTech). Human lung microsomes were obtained from a pool of five individuals (Cat # HPM 501, Lot 1.0, Human Biologics International, Scottsdale, AZ). Human liver cytosol was obtained from a mixed pool of 15 individuals (Lot# HHC 280, Tissue Transformation Technologies, Edison, NJ). Human lung cytosol was from a single male (Lot # HG714100, Tissue Transformation Technologies). Human donor demographic information and metabolic characterization is available but not reported here for the sake of brevity.

Microsomal hydrolysis of 1-CEO. The time course of 1-CEO metabolism was measured in liver and lung microsomes from each species by further refinement of the method described in Himmelstein *et al.* (2001a). Vials (1 ml liquid/10 ml vial) were prepared with 0.1 M phosphate buffer (pH 7.4), MgCl$_2$, (15 mM), EDTA (0.1 mM), glucose-6-phosphate (0.8 mM), and glucose-6-phosphate dehydrogenase (1 U/ml). The vials were sealed with crimp top, Teflon®-coated silicone septa (Gerstel US, Baltimore MD) with a Parafilm™ sheet between the metal crimp top and septa and plastic tape around the outside rim of the crimp top to insure a positive seal. Incubations were performed using a programmable x-y-z robotic multi-purpose gas chromatograph (GC) sampler (MPS2, Gerstel, Baltimore, MD). Sample vials were transferred to the MPS2 agitator-heater block and preheated for 11 min at 500 rpm. Known concentrations of 1-CEO (prepared in Tedlar bags) were added by manually flushing the vial headspace with approximately 15 ml of vapor (see Fig. legends for actual concentrations used). The headspace concentration was immediately quantified by robotic transfer from the vial to the GC inlet, using the MPS2 1.0 ml

gas-tight syringe. The optimal syringe temperature (38°C), sample injection volume (200 µl), and injection speed (800 µl/s) were pre-determined experimentally. The protein concentration (0.25–3 mg/ml) and duration of incubation (0–60 min) were also optimized during preliminary experiments. Microsomal protein for the definitive experiments (10–50 µl to final concentration of 0.5 mg/ml) was manually added to the vial to start the enzymatic time course reactions. Between injections, the headspace-sampling syringe was flushed with helium (at 48.5°C for 3 min) to clear residual chemical. Prior to the next sample (t = 12 min), an injection of air was made to check for residual chemical, which if present, was subtracted from the next headspace sample. The air, sample injections, and syringe flushes were repeated (t = 12, 24, 36, 48, and 60 min) to determine the time course of metabolism. Control incubations included phosphate buffer or heat-inactivated microsomes. The concentration of 1-CEO in vial headspace was calculated using linear regression analysis from gasbag standards. Headspace GC-mass spectrometry (GC/MS) analysis by single ion monitoring (m/z 39/1-CEO) was conducted as described previously (Himmelstein *et al.*, 2001a). The limit of quantification of 1-CEO (and CD in subsequent experiments described below) was 0.001 nmol/ml of headspace (equivalent to 24 ppb).

Microsomal oxidation of 1-CEO. Vials were prepared with incubation reagents as described above. Cofactor NADP$^+$ was added to the vial 10 s before the addition of microsomal protein. Time-course data for 1-CEO, with and without NADP$^+$, were measured over a range of starting 1-CEO concentrations. In mouse liver microsomes, the only species to show significant metabolism, additional incubations were conducted in the presence of 4-methylpyrazole (4-MP) or 1-aminobenzotriazole (ABT) as inhibitors of cytochrome P450-dependent oxidation (Halpert *et al.*, 1994). Stock solutions (100 mM) of 4-MP in phosphate buffer or ABT in acetonitrile were added to a final concentration of 100 µM; control incubation mixtures included equal amounts of buffer or acetonitrile. Additional incubations were conducted to isolate the potential oxidative metabolite of 1-CEO. Incubation mixtures containing mouse liver microsomes were agitated in a Bucher shaker (Labconco, Lenexa, KS) at 37°C with 1-CEO (10 mM) in 10 ml total volume in sealed 24 ml vials, with or without NADP$^+$. After 30 min, the reactions were stopped by the addition of cold ethyl acetate (10 ml) and NaCl (5 g/vial). Following centrifugation (1700 × g for 5 min) and extraction with ethyl acetate (10 ml, then 5 ml), the solvent was analyzed by full scan GC/MS. Instrument conditions were similar to those used previously (Cottrell *et al.*, 2001).

Cytosolic GSH conjugation of CD or 1-CEO. Preliminary experiments showed no reactivity of CD with GSH in cytosol or heat-inactivated cytosol. For 1-CEO, the incubation vials were prepared as described above for the microsomal 1-CEO hydrolysis experiments, except that cytosolic protein from each species (1–2 mg protein/ml) and GSH (10 mM) were used. Headspace samples (400 µl) were taken at 0, 12, 24, 36, 48, and 60 min, after the reactions were started by the addition of cytosol and GSH. Control incubations in phosphate buffer were conducted using 1-CEO alone, 1-CEO + GSH, and 1-CEO + GSH + heat-inactivated cytosol.

Microsomal oxidation of CD. The time course of CD disappearance and 1-CEO formation and hydrolysis was measured simultaneously in liver or lung microsomes. For liver microsomal incubations from each species, vials were prepared with the incubation reagents described above for microsomal 1-CEO hydrolysis. After preincubation (37°C for 5 min), an equal volume of vial headspace was removed from the vial and replaced with known concentrations of CD vapor. The vial was equilibrated for approximately 10 min, and reactions were started by the addition of microsomal protein (1 mg/ml) and NADP$^+$ (0.4 mg/ml of suspension). The protein concentration was optimized during preliminary experiments (0.5–3.0 mg/ml). Control incubations were performed without NADP$^+$ or with NADP$^+$ and heat-inactivated microsomes. Incubation start times were staggered, and up to five vials per exposure concentration were used to describe the time course of headspace 1-CEO relative to the disappearance of CD from the headspace. The repeated headspace samples (400 µl, 4–6 injections per vial) were analyzed at 12-min intervals for up to 1 h by GC/MS. For lung microsomes, the incubation conditions were identical to those used for liver microsomes except for the

different starting CD concentrations. For some incubations, 4-MP or ABT (at final concentrations of 100 μM) were added to determine if CD oxidation was dependent on cytochrome P450-monooxygenase.

Model development. A two-compartment model was used to describe the distribution and metabolism of CD and 1-CEO in the closed vial system. Mass transport between the air and liquid phases was assumed to be instantaneous, and thus partition coefficients were used to describe distribution between phases. The liquid-to-air volume ratio (1-to-10) was small, and the liquid was stirred vigorously to ensure rapid mixing during preincubation and reaction periods (described above). A known volume of air containing a fraction of the air phase CD and 1-CEO was removed from the system at each sampling time. Experiments with PBS buffer or heat-inactivated microsomes were used to calculate the control loss from the vial system. The measured concentrations of CD and 1-CEO in the air phase and their known liquid-to-air partition coefficients (0.69 for CD and 57.9 for 1-CEO; Himmelstein *et al.*, 2001a) were used to calculate the liquid phase concentrations. Given the control loss, the model was used to calculate the rate constants for 1-CEO hydrolysis, further 1-CEO oxidation if present, CD oxidation, and GSH conjugation. Microsomal 1-CEO hydrolysis and total CD oxidation were parameterized as Michaelis-Menten-type equations. The 1-CEO formed by CD oxidation was parameterized, initially using the constants for total CD oxidation and the 1-CEO hydrolysis constants previously calculated. For cases where 1-CEO concentrations were over-predicted, the model predictions were reduced by dividing the total CD oxidation into two pathways: one parameterized from the 1-CEO formation, and the other from total CD disappearance, representing metabolism to uncharacterized products. Disappearance of 1-CEO from the headspace was used to quantify the conjugation of 1-CEO with cytosolic GSH. Non-enzymatic conjugation was simulated as a first-order reaction and enzymatic conjugation was simulated as a pseudo second-order process involving GST-mediated conjugation of 1-CEO with GSH and binding of 1-CEO directly with the enzyme.

The differential equations describing the model, along with the detailed nomenclature, are given in the appendix (see Supplementary Data). Model simulation was conducted using the Advanced Continuous Simulation Language (ACSL version 11.8.4, Aegis Technologies Group, Huntsville, AL). Parameter optimization was conducted using ACSL Math and Optimize version 2.5.4 (Aegis Technologies Group). All of the model metabolic parameters were optimized in ACSL-Optimize, using the Nelder-Mead method and a relative error minimization-based, log-likelihood function. For pathways with more than one metabolic constant, the parameters were optimized simultaneously to avoid local log-likelihood minima. The model code is available upon request.

RESULTS

Microsomal Oxidation of CD

Total CD oxidation in liver microsomes among the species and strains tested was described as a saturable Michaelis-Menten mechanism (Fig. 1, Table 1). Comparison of the kinetic rates as Vmax/Km (ml/h/mg protein) suggests that intrinsic clearance was mouse $\approx$ hamster > Fischer rat $\approx$ Wistar rat > human. The time course of CD oxidation was also saturable in mouse lung microsomes (Fig. 2). CD oxidation by rat, hamster, and human lung microsomes appeared saturated at all test concentrations; the rate was optimized as Vmax/Km rather than independent values of Vmax and Km. The intrinsic clearance in lung microsomes based on Vmax/Km was mouse >> Fischer rat $\approx$ Wistar rat $\approx$ hamster $\approx$ human.

Microsomal Hydrolysis of 1-CEO

1-CEO was resistant to non-enzymatic hydrolysis based on the slow rate of loss from headspace in the presence of phosphate buffer (Fig. 3A); the loss was the same with or without heat-inactivated microsomes. Saturable Michaelis-Menten metabolism of 1-CEO was evident, especially in hamster and human liver and lung microsomes (Figs. 3B and 3C, Table 2). The Vmax values ranged from 0.14 to 3.66 μmol/h/mg protein in liver microsomes; the apparent Km values ranged from

FIG. 1. Oxidative metabolism of CD in liver microsomes: (A) control loss in phosphate buffer for starting CD headspace concentrations ranging from 0.02 to 22 nmol CD/ml. Saturable metabolism is evident in B–D, showing experimental data (symbols) and model simulations (solid lines) for the mouse at starting CD headspace concentrations of 0.41–22 nmol/ml (B), hamster at 2–22 nmol/ml (C), and pooled human liver microsomes at 2–11 nmol/ml (D). Data for Wistar and Fischer rats at 2–11 nmol/ml (not shown) had curves similar in shape to human. Concentration of 1 nmol gas/ml is approximately equal to 24 ppm.
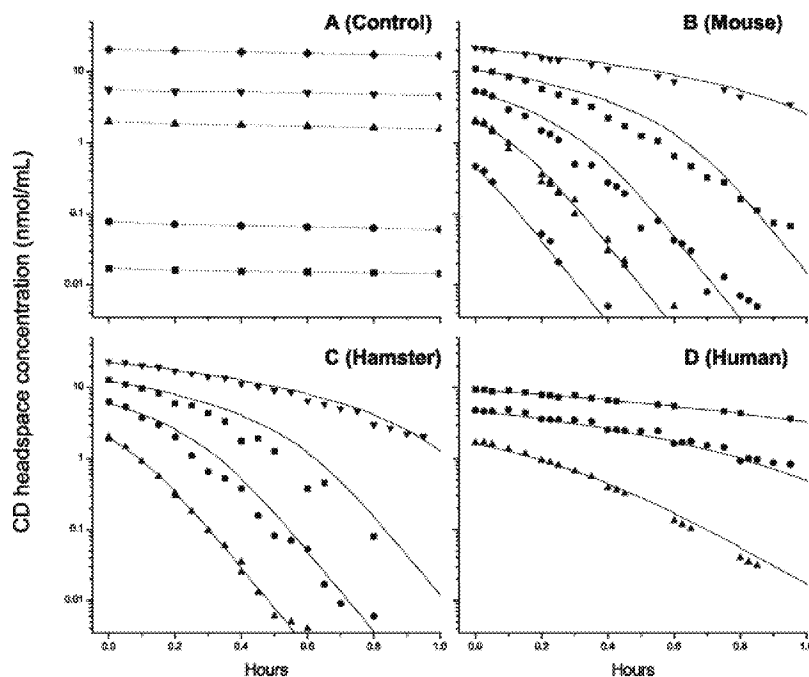
TABLE 1
Optimized Parameters for Microsomal Oxidation of β-chloroprene (CD)

Tissue	Species	Activity of microsomal oxidation		
		Vmax	Km	Vmax/Km
Liver	Mouse	0.23	1.03	224
	Fischer rat	0.078	0.53	146
	Wistar rat	0.11	0.84	125
	Hamster	0.29	1.33	218
	Human	0.068	0.68	101
Lung	Mouse	0.10	1.5	66.7
	Fisher rat	—	—	1.3[a]
	Wistar rat	—	—	1.3[a]
	Hamster	—	—	1.3[a]
	Human	—	—	1.3[a]

Note. Derived from modeling of vial headspace concentration time-course data using a liquid-to-air partition coefficient of 0.69 (Himmelstein *et al.*, 2001a). Vmax, μmol/h/mg protein; Km, μmol/l; Vmax/Km, ml/h/mg protein.

[a]The apparent rate of lung metabolism, over the range of biologically relevant concentrations tested, was linear and was estimated as Vmax/Km.

20.9–99.7 μM (Table 2). Vmax/Km values (ml/h/mg protein) were lowest in mouse < rat < hamster ≈ human. Similar species differences were obtained for lung microsomes with Vmax ranging from 0.11 to 1.34 μmol/h/mg protein and Km from 51.5 to 187.6 μM. The lung Vmax/Km values (ml/h/mg protein) were mouse ≈ rat < hamster ≈ human.

Microsomal Oxidation of 1-CEO

Hydrolysis experiments conducted in the presence and absence of NADP$^+$ indicated additional metabolism in B6C3F1 mouse liver microsomes but not in human, rat, or hamster liver
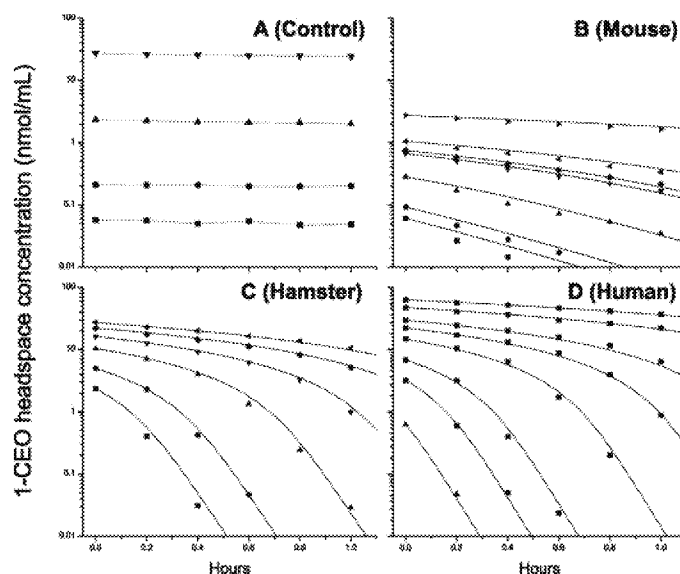
FIG. 3. Epoxide hydrolase-dependent concentration time course of headspace 1-CEO in liver microsome incubations: (A) Buffer control data (symbols with dashes) showing minimal loss due to spontaneous hydrolysis and repeated sampling; buffer control data were indistinguishable from heat-inactivated microsomes (data not shown). Representative experimental data (symbols) and model simulations (lines) are shown for (B) mouse, (C) hamster, and (D) pooled human liver. Time-course data for Wistar and Fischer rats (not shown) were similar to other species presented. Starting concentrations ranged from 0.37 to 330 nmol/ml. Similar time course experiments and results were obtained using lung microsomes and starting concentrations of 0.37–250 nmol/ml (data not shown).

microsomes; representative data are presented for mouse and human (Fig. 4). Pretreatment of the microsomal suspension with 4-MP or ABT inhibited oxidation but did not affect hydrolysis (Fig. 4A). The rate of 1-CEO hydrolysis in mouse
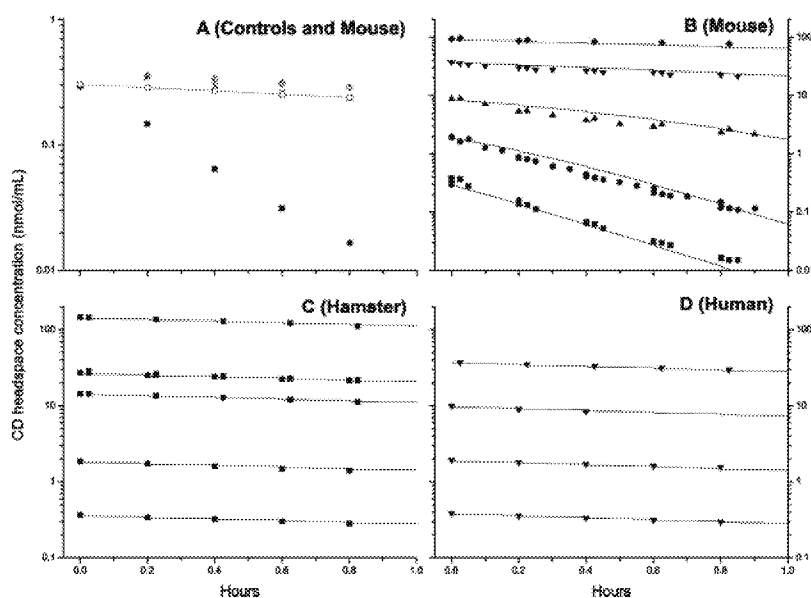
FIG. 2. Oxidative metabolism of CD in lung microsomes: (A) Experimental data showing decline of CD headspace concentration with B6C3F1 mouse lung microsomes with NADP$^+$ (■) and lack of decline without NADP$^+$ (◇ open diamond) or with the P450 inhibitors aminobenzatrizole (+) or 4-methylpyrazole (×) relative to phosphate buffer (- -□- -); (B) mouse experimental data (■ solid square, ● solid circle, ▲ solid up triangle, ▼ solid down triangle, ◆ solid diamond) and model simulations (solid lines ——) at starting CD headspace concentrations of 0.41, 2.0, 10, 41, or 409 nmol/ml, respectively; (C) hamster (■ solid square) at 0.41, 2.0, 20, 41, or 410 nmol/ml, and (D) pooled human lung microsomes (▼ solid down triangle) at 0.41, 2.0, 11, or 41 nmol/ml. Time-course data for Fischer rats at 0.41 or 41 nmol CD/ml and Wistar rats at 0.41, 2.0, or 41 nmol/ml (not shown) were similar to hamster and human data.

TABLE 2
Optimized Parameters for Microsomal Epoxide Hydrolase Activity of (1-chloroethenyl)oxirane (1-CEO)

Tissue	Species	Activity of microsomal epoxide hydrolase		
		Vmax	Km	Vmax/Km
Liver	Mouse	0.14	20.9	6.7
	Fischer rat	0.60	41.5	14.5
	Wistar rat	0.64	53.0	12.1
	Hamster	2.49	73.8	33.7
	Human	3.66	99.7	36.7
Lung	Mouse	0.11	51.5	2.1
	Fischer rat	0.12	90.9	1.3
	Wistar rat	0.16	91.6	1.7
	Hamster	1.34	187.6	7.1
	Human	0.58	72.2	8.0

Note. Derived from modeling of vial headspace concentration time course data using a liquid-to-air partition coefficient of 57.9 (Himmelstein *et al.*, 2001a). Vmax, μmol/h/mg protein. Km, μmol/l; Vmax/Km, ml/h/mg protein.

liver microsomes was optimized independently from the previous hydrolysis experiment (Fig. 3), giving a Vmax of 0.54 μmol/h/mg protein and an apparent Km of 85.4 μM. The derived Vmax/Km was 6.0 ml/h/mg protein, comparable to the value of 6.7 obtained in the previous experiment (Table 2). A faster rate of *in vitro* metabolism was observed in the presence of NADP$^+$ for mice but not for humans (Figs. 4B and 4C). The rate of oxidation was proportional to the concentration of protein (0.5 and 1.0 mg/ml) (data not shown). The Vmax for oxidative metabolism of 1-CEO was 0.39 μmol/h/mg protein and the apparent Km was 16.8 μM; intrinsic clearance was 23

ml/h/mg protein. An experiment conducted to identify the potential oxidative metabolite(s) of 1-CEO in mouse liver microsomes revealed only the diol metabolite of 1-CEO, 3-chloro-3-butene-1,2-diol, by full-scan mass spectrometry (data not shown). Presence of the diol was consistent with data reported by Cottrell *et al.* (2001). The potential for 1-CEO oxidative metabolism in lung microsomes was not evaluated.

Time Course of 1-CEO Formation from CD

The cytochrome P450-dependent oxidation of CD in liver and lung microsomes was accompanied by the appearance of 1-CEO in the headspace (Figs. 5 and 6). Peak headspace concentrations of 1-CEO ranged from approximately 0.01 to 0.1 nmol/ml for liver microsomes. In liver, the faster rate of total CD oxidation for the B6C3F1 mouse was commensurate with a greater production of 1-CEO when compared with rat, hamster, or human (Figs. 5A–5E). A clear CD dependent increase in 1-CEO formation was evident in mouse lung microsomes with peak headspace concentrations comparable to mouse liver microsomes (Fig. 6A). Despite the low total oxidation of CD, 1-CEO could still be quantified in rat and hamster lung microsome incubations (Figs. 6B–6D). For the human lung microsomes, only one detectable value of 1-CEO was recorded early in the incubation with 41 nmol CD/ml, most likely because of the relatively high rate of removal by epoxide hydrolase (Table 2). The kinetic parameters describing the 1-CEO time-course data are presented in Table 3. Interpretation of the model simulations is provided in the *Discussion.*

Conjugation of 1-CEO with GSH

Like the 1-CEO hydrolysis experiments above, the minimal rate of decline of 1-CEO in phosphate buffer was combined
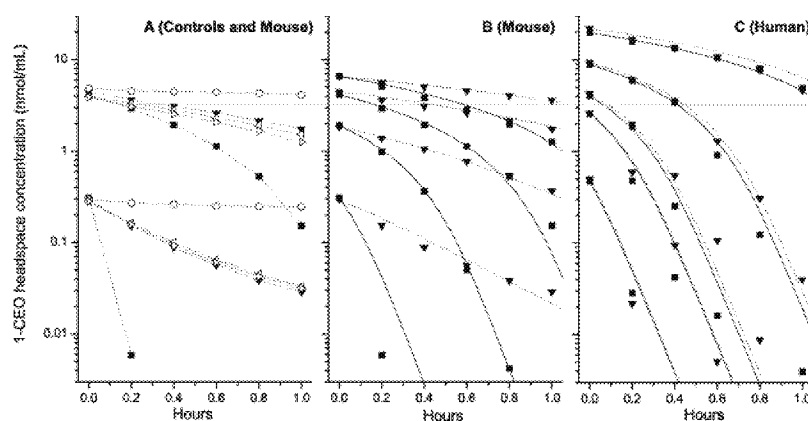

FIG. 4. Cytochrome P450 and epoxide hydrolase-dependent time course of headspace 1-CEO concentration in liver microsome incubations: (A) Experimental data for 1-CEO in buffer as control (○ open circle), mouse liver microsomes without NADP$^+$, (▼ solid down triangle), with NADP$^+$ (■ solid square), and with NADP$^+$ and cytochrome P450 oxidase inhibitors 4-MP (△ open up triangle) or ABT (▽ open down triangle), respectively; starting 1-CEO concentrations were 2.1 or 21 nmol 1-CEO/ml. (B) Mouse liver microsomes showing model (dashed and solid lines) and experimental data for 1-CEO without NADP$^+$ (▼ solid down triangle) or with NADP$^+$ (■ solid square); starting concentration range was 2.1–31 nmol 1-CEO/ml. (C) Pooled human liver microsomes showing model and experimental data indicating similar metabolism with and without NADP$^+$; starting concentration range 4.1–165 nmol 1-CEO/ml. Results for human were similar for other rodents (data not shown for Fischer rat, Wistar rat, or Syrian hamster).
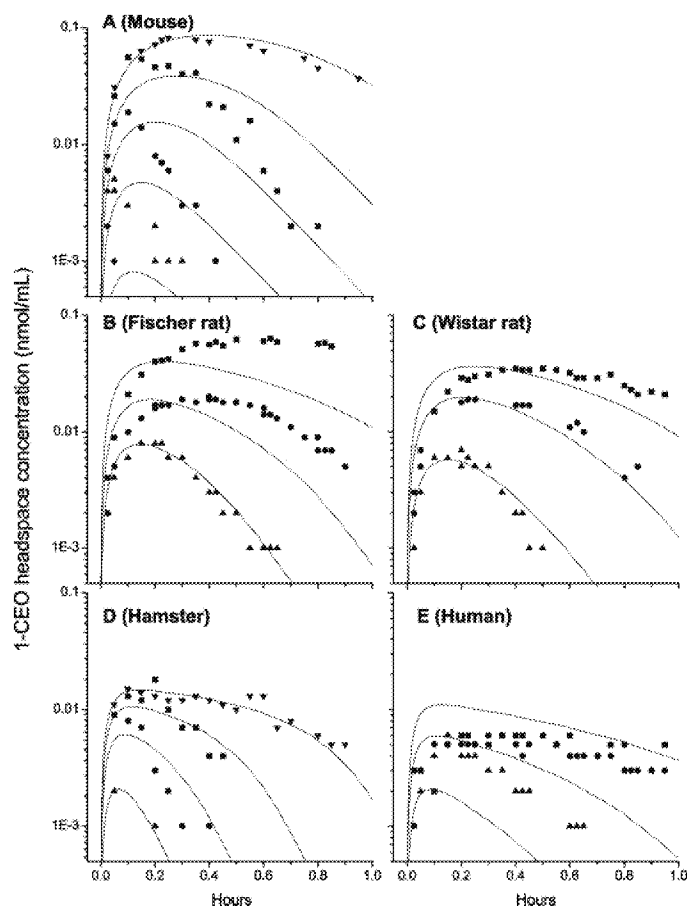
FIG. 5. Time course of 1-CEO formation from CD in liver microsomes: Experimental data (symbols) and model simulations (lines) for 1-CEO corresponding to CD oxidation presented in Figure 1. All species are presented: (A) mouse, (B) Fischer rat, (C) Wistar rat, (D) hamster, and (E) human.
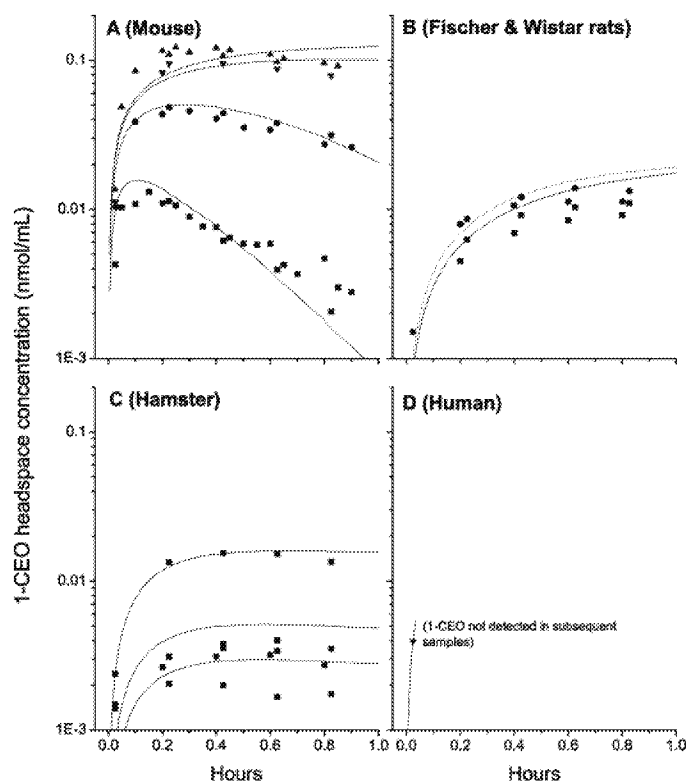

FIG. 6. Time course of 1-CEO formation from CD in lung microsomes: Experimental data (symbols) and model simulations (lines) for 1-CEO corresponding to CD oxidation presented in Figure 2: (A) mouse at starting CD headspace concentrations of 2.0, 10, 41, or 409 nmol/ml, (B) Fischer (—, solid line) and Wistar (dashed line) rats at 41 nmol/ml, (C) hamster at 20, 41, 410 nmol/m;, and (D) pooled human lung microsomes at 41 nmol/ml for which 1-CEO was detected only at one early time point.

with losses due to repeated sampling. The nonenzymatic first-order GSH reaction rate ($kf = 0.7$ h^{-1}) with 1-CEO in buffer was equivalent to the rate of 1-CEO reaction with GSH in heat-inactivated cytosol (Fig. 7). The data were best described by a pseudo-second order mechanism modeled with the rate constant (ks, $1/\mu mol/h/mg$ protein) and the initial concentration of reactive sites ($C^{BS(0)}$, $\mu mol/l$). Enzymatic clearance of 1-CEO was described as $ks \cdot C^{BS(0)} = /h/mg$ protein (Table 4). The fastest rate for liver cytosol was observed in the hamster > Fischer rat $\approx$ Wistar rat > mouse > human; the overall difference between the hamster and human was about eight-fold. In lung cytosol, the rates were mouse > Fischer rat > human > Wistar rat > hamster, with a four-fold difference between mouse and hamster.

DISCUSSION

The initial step in CD metabolism is cytochrome P450-dependent oxidation to the epoxide metabolite, 1-CEO and 2-chloro-2-ethenyloxirane (2-CEO), the latter of which was

TABLE 3

Kinetic Parameters Used to Describe Time Course of (1-chloroethenyl)oxirane (1-CEO) from Microsomal Oxidation of β-chloroprene (CD)

Tissue	Species	1-CEO formation[a]			Ratio of 1-CEO/ total (%)[b]
		Vmax	Km	Vmax/Km	
Liver	Mouse	0.149	36.6	4.1	2
	Fischer rat	0.184	23.7	7.8	5
	Wistar rat	0.148	25.3	5.8	5
	Hamster	0.048	9.0	5.4	2
	Human	0.108	20.7	5.2	5
Lung	Mouse	0.050	25.0	2.00	3
	Fischer rat	0.0075	40.4	0.19	15
	Wistar rat	0.0082	30.1	0.27	22
	Hamster	0.013	81.2	0.16	13
	Human	0.024	24.6	0.98	78

[a]Optimized oxidative rate constants used to describe the amount of 1-CEO derived from total CD oxidation.

[b]Vmax/Km for 1-CEO formation divided by the Vmax/Km for total CD oxidation (from Table 1) multiplied by 100%.

FIG. 7. Glutathione S-transferase re-activity with 1-CEO in liver cytosol: (A) Time course of 1-CEO in pooled human cytosol with GSH (■ solid square, ● solid circle, ▲ solid up triangle and ▼ solid down triangle representing starting 1-CEO headspace concentrations equivalent to 0.41, 4.1, 41, or 550 nmol/ml), human boiled cytosol with GSH (×), 1-CEO with GSH (+), and phosphate buffer without GSH (- -□- -). Representative experimental data (symbols) and model (lines) for (B) human, (C) mouse, and (D) hamster cytosol; time course data for Fischer and Wistar rat are not shown. Similar experiments were conducted with lung cytosol using starting concentrations of 0.37–250 nmol 1-CEO/ml (data not shown).
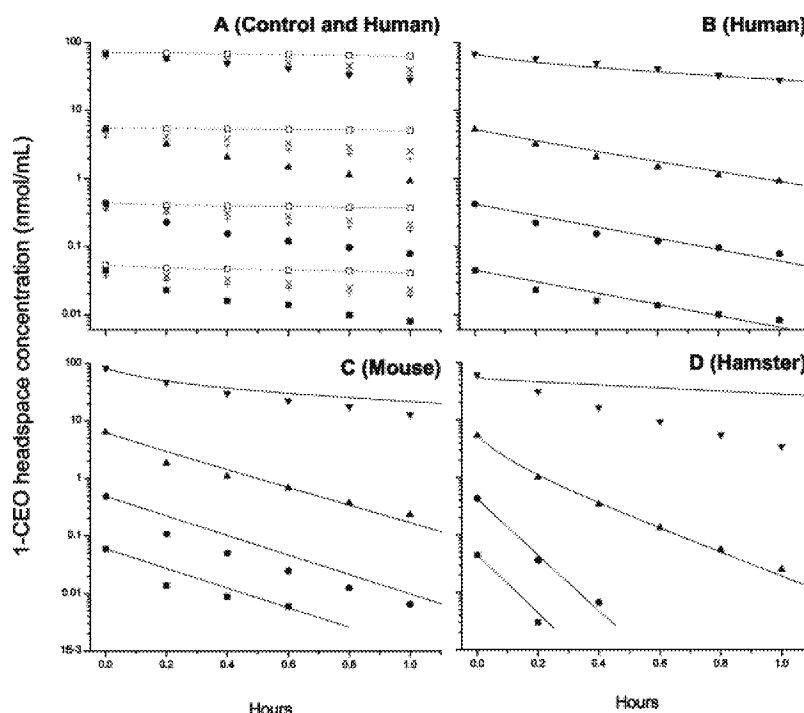
inferred based on the detection of further hydrolysis products of 2-CEO (Cottrell *et al.*, 2001). The instability of 2-CEO in aqueous media (Cottrell *et al.*, 2001) is consistent with that of chloroethyloxirane from vinyl chloride (Ghissassi *et al.*, 1998). Because of its instability, quantification of 2-CEO formation in the current study was not possible. The stability of 1-CEO is

TABLE 4
Optimized Parameters for Cytosolic Glutathione S-transferase Activity toward (1-chloroethenyl)oxirane (1-CEO)

Tissue	Species	Activity of cytosolic glutathione S-transferase[a]		
		ks	$C^{BS(0)}$	ks · $C^{BS(0)}$
Liver	Mouse	0.0015	2.7	0.0040
	Fischer rat	0.0074	0.92	0.0068
	Wistar rat	0.011	0.56	0.0063
	Hamster	0.024	0.54	0.0130
	Human	0.0017	0.94	0.0016
Lung	Mouse	0.0011	2.01	0.0022
	Fischer rat	0.0023	0.70	0.0016
	Wistar rat	0.0051	0.18	0.00092
	Hamster	0.015	0.038	0.00056
	Human	0.0028	0.44	0.0012

Note. ks (l/μmol/h/mg cytosolic protein), rate constant $C^{BS(0)}$ (μmol/l) as initial concentration of protein binding sites and ks · $C^{BS(0)}$ (h/mg protein) describing enzymatic 1-CEO-GSH conjugate formation as a pseudo-second order reaction.

[a] First order reaction of 1-CEO with GSH was measured as kf = 0.07 h^{-1} independent of protein.

consistent with oxirane from ethylene, epoxybutene from butadiene, or isoprene monoepoxides from isoprene (Csanády *et al.*, 2000; Malvoisin *et al.*, 1979; Schmiedel *et al.*, 1983; Watson *et al.*, 2001). Our preliminary experiments identified 1-CEO as a cytochrome P450-dependent metabolite of CD, and showed that microsomal epoxide hydrolase-mediated hydrolysis and cytosolic GST-mediated GSH conjugation were involved in the *in vitro* metabolism of 1-CEO (Himmelstein *et al.*, 2001a). As a consequence of the chemical instability of 2-CEO, our efforts focused on the quantification of CD oxidation and the elimination reactions of 1-CEO. The results presented here provide quantitative interspecies comparisons of CD oxidation and the 1-CEO metabolic steps.

Oxidative Metabolism of CD

CD metabolism by liver microsomes was similar across species with intrinsic clearance showing a maximum difference of about two-fold greater in the mouse than the human. The results were consistent with recent findings for CD oxidation in microsomal liver preparations with mice > rats > humans (Munter *et al.*, 2003). Comparison of results for CD and 1,3-butadiene (a nonchlorinated chemical analog) is possible given the similar experimental approach. The Vmax/Km values for microsomal CD oxidation appear to be faster than those reported for the oxidation of butadiene to epoxybutene (Csanády *et al.*, 1992). For example, the range of maximum rates (μmol/h/mg protein) for CD (0.068 to 0.29) was similar to butadiene (0.04 to 0.16). However, the corresponding apparent Km constants for CD (0.53 to 1.33 μM) suggest slightly

greater affinity of CD for cytochrome P450 compared with butadiene (2 to 5.1 μM). The Vmax/Km for butadiene in liver microsomes was mouse (78) > human (14) > rat (9), all lower compared with the Vmax/Km values for CD (Table 1).

Oxidation rates for CD and butadiene also were comparable for lung microsomes. The Vmax values for CD and butadiene were 0.1- and 0.14-μmol/h/mg protein, respectively; the corresponding apparent Km values were 1.5 and 5 μM. The intrinsic clearance for total CD oxidation was greater for the mouse (66.7) when compared to the other species (1.3). For butadiene, the Vmax/Km values in the lung microsomes were mouse (28) > human (4.5) ≈ rat (1.2). The differences in the Vmax/Km values for CD and BD in the mouse appear consistent with the relatively greater potency of CD than butadiene for lung tumors, although species sensitivity differences may also be due to tissue concentration differences caused by chemical partitioning. For example, the lowest exposure concentration that produced lung tumors in male mice was 12.8 ppm CD compared with 62.5 ppm for butadiene (Melnick *et al.*, 1999).

Microsomal Hydrolysis of 1-CEO

The liquid-to-air partition coefficient for 1-CEO (58:1) used for predicting the rate of metabolism in microsomal suspensions was similar to oxirane (77:1) (Schmiedel *et al.*, 1983). The Vmax/Km for 1-CEO hydrolysis in liver microsomes indicated that mice were about two times slower than rats and six times slower than hamsters or humans. The apparent Km values were consistent with those published for other oxirane analogs such epoxybutene, oxirane, and propylene oxide, although there appear to be differences in Vmax for these different substrates (Csanády *et al.*, 1992; Brown *et al.*, 1996; Faller *et al.*, 2001; Krause *et al.*, 1997; Kreuzer *et al.*, 1991). A previous study also established that 1,1,1-trichloropropene oxide (TCPO), a competitive substrate of epoxide hydrolase, inhibited this reaction (Himmelstein *et al.*, 2001a). The product formed in the absence of inhibition was 3-chloro-3-butene-1,2-diol (Cottrell *et al.*, 2001).

Microsomal Oxidation of 1-CEO

This reaction in liver microsomes appeared to be limited to mouse, and was not evident in liver microsomes from human, rat, or hamster. In the case of 1,3-butadiene metabolism, a faster rate of epoxybutene oxidation to diepoxybutane has been observed in mouse liver microsomes compared with the rat or human (Csanády *et al.*, 1992). The intrinsic clearance of 1-CEO by oxidation in mouse liver microsomes (23 ml/h/mg protein) was approximately 10-fold less than the clearance of CD oxidation (224 ml/h/mg protein). It is not yet known if oxidative metabolism of 1-CEO occurs in mouse lung. The dependence of the reaction on NADP$^+$ and inhibition by 4-MP or ABT clearly suggests involvement of cytochrome P450 monooxygenase. Oxidation of 1-CEO by the mouse potentially could lead to a reactive intermediate such as a diepoxide, but

our results (data not shown) confirmed the diol hydrolysis product of 1-CEO previously reported (Cottrell *et al.*, 2001). Cottrell *et al.* (2001) reported that a synthetic standard of chloroprene diepoxide was chemically unstable in aqueous media, forming products that have yet to be characterized.

Kinetics of CD and 1-CEO

To our knowledge, this is the first example of simultaneous time-course analysis of a parent chemical and its metabolite, either for CD or for similar chemical analogs. The 1-CEO time course initially was modeled as if it was the sole product of CD, but this approach indicated that 1-CEO formation with subsequent hydrolysis represented a fraction of the total CD oxidation occurring *in vitro*. Because 2-CEO was unstable in aqueous media and could not be quantified, a determination of the mass balance between the two epoxide-formation pathways was not possible. However, a satisfactory description of the 1-CEO time course data was obtained by modeling a split of the cytochrome P450-dependent CD oxidative metabolite leading to 1-CEO and other uncharacterized product(s), while using the measured 1-CEO epoxide hydrolase kinetics to account for 1-CEO elimination (Fig. 5). The formation of 1-CEO was best described as representing 2–5% of the total oxidative metabolism of CD across the animals tested (Table 3). Results similar to those presented in Figure 5 were also obtained by re-optimizing the rates of 1-CEO hydrolysis so that the rate of 1-CEO removal was substantially increased. This alternative model description was considered inappropriate because 1-CEO epoxide hydrolase activity was experimentally measured. The finding that the majority of CD oxidation leads to metabolites other than 1-CEO warrants further investigation as these metabolites may be important to understanding relative tumorigenicity across species.

Adjustment of 1-CEO formation as a proportion of total CD oxidation in lung microsomes was less robust than that for the liver because of the limited amount of 1-CEO time course data (Fig. 6). In rodents, estimates of adjusted Vmax/Km were 3–22% of the total oxidative CD metabolism (Table 3). The value of 78% for human lung microsomes likely represents an overestimation because of rapid removal of 1-CEO by epoxide hydrolase. An inherent limitation of estimating *in vitro* metabolism using microsomes prepared from whole lungs is the distribution of different cell types and low enzyme activity in the homogenized lung tissue (Plopper *et al.*, 1991, Seaton *et al.*, 1996). Despite this shortcoming, the greater CD oxidation and 1-CEO formation in the mouse compared with the other rodents provides some insight regarding the greater tumor response of this tissue in the B6C3F1 mouse.

Cytosolic Metabolism of 1-CEO

The experimental approach was similar to that used to describe GST-mediated metabolism of 1,2-epoxy-3-butene and propylene oxide (Faller *et al.*, 2001; Kreuzer *et al.*, 1991). The

half-life for the spontaneous first-order reaction between 1-CEO and GSH was approximately 10 h. This appears to be longer than the half-lives for spontaneous GSH reactivity with propylene oxide of 1.7 h (Faller *et al.*, 2001), and epoxybutene (3.9 h, Csanády *et al.*, 1992; 0.8 h, Kreuzer *et al.*, 1991). The enzymatic pseudo-second order reaction between 1-CEO and GSH suggests greater GST capacity in liver than lung. Enzymatic GSH conjugation with 1-CEO was first thought to be a standard saturable Michaelis-Menten reaction but a closer analysis of the data showed divergent behavior. In particular, the conjugation rate at a given concentration was dependent on the starting concentration (Fig. 7D). For example, the rate in hamster liver cytosol for the 4.1 nmol/ml starting 1-CEO headspace concentration was faster than at 41 nmol/ml. Standard Michaelis-Menten kinetics would have shown approximately parallel data. This behavior suggested that active enzymatic sites were being consumed rather than following standard Michaelis-Menten kinetics. The description of this enzymatic reaction as pseudo second order is consistent with the known irreversible binding of substrate with some forms of GST (Raham *et al.*, 1999). Numerous other epoxides, such as oxirane, propylene oxide, epoxybutene, diepoxybutane, also undergo metabolism by GST (Brown *et al.*, 1996; Faller *et al.*, 2001; review by Himmelstein *et al.*, 1997). Additional research is needed to identify the structures of the GSH conjugates and the potential impact of GSH depletion on *in vivo* toxicity.

Conclusions

Total CD oxidation was evident in liver and lung microsomal tissue fractions. Species and tissue differences were observed, the most dramatic of which was a faster rate of CD metabolism in the mouse lung compared with the other species. The time course data for simultaneous microsomal metabolism of CD and 1-CEO were explained by formation of 1-CEO and uncharacterized products; across species 1-CEO formation in the liver fraction appeared to be 2–5% of the total CD oxidation. The findings support the need for better understanding of the kinetic relationship between oxidative formation of epoxide metabolites and their elimination by epoxide hydrolase for analogs such as butadiene, β-chloroprene, and isoprene. Cytosolic GST-mediated conjugation was quantified as a pathway for 1-CEO metabolism. Overall, the *in vitro* kinetic parameters developed here improve the understanding of CD metabolism. The kinetics of total CD oxidation measured in liver and lung microsomes have been used to develop a physiologically based toxicokinetic model to aid in CD risk assessment (Himmelstein *et al.*, 2004).

REFERENCES

Acquavella, J., and Leonard, L. (2001). Review of epidemiologic research on 1,3-butadiene and chloroprene. *Chem. Biol. Interact.* **135–136**, 43–52.

Bartsch, H., Malaveille, C., Barbin, A., and Planche, G. (1979). Mutagenic and alkylating metabolites of halo-ethylenes, chlorobutadienes, and dichlorobutenes produced by rodent or human liver tissues: Evidence for oxirane formation by P450-linked microsomal monooxygenases. *Arch. Toxicol.* **41**, 249–277.

Brown, C. D., Wong, B. A., and Fennell, T. R. (1996). *In vivo* and *in vitro* kinetics of ethylene oxide metabolism in rats and mice. *Toxicol. Appl. Pharmacol.* **136**, 8–19.

Colonna, M., and Laydevant, G. (2001). A cohort study of workers exposed to chloroprene in Department de l'Isere, France. *Chem. Biol. Interact.* **135–136**, 505–514.

Cottrell, L., Golding, B. T., Munter, T., and Watson, W. P. (2001). *In vitro* metabolism of chloroprene: Species differences, epoxide stereochemistry, and a de-chlorination pathway. *Chem. Res. Toxicol.* **14**, 1552–1562.

Csanády, G. A., Denk, B., Putz, C., Kreuzer, P. E., Kessler, W., Baur, C., Gargas, M. L., and Filser, J. G. (2000). A physiological toxicokinetic model for exogenous and endogenous ethylene and ethylene oxide in rat, mouse, and human: Formation of 2-hydroxyethyl adducts with hemoglobin and DNA. *Toxicol Appl Pharmacol.* **165**, 1–26.

Csanády, G. A., Guengerich, F. P., and Bond, J. A. (1992). Comparison of the biotransformation of 1,3-butadiene and its metabolite, butadiene monoepoxide, by hepatic and pulmonary tissues from humans, rats, and mice. *Carcinogenesis* **13**, 1143–1153; Erratum in: *Carcinogenesis* **14**, 784.

Drevon, C., and Kuroki, T. (1979). Mutagenicity of vinyl chloride, vinylidene chloride, and chloroprene in V79 Chinese hamster cells. *Mutat. Res.* **67**, 173–182.

Faller, T. H., Csanády, G. A., Kreuzer, P. E., Baur, C. M., and Filser, J. G. (2001). Kinetics of propylene oxide metabolism in microsomes and cytosol of different organs from mouse, rat, and human. *Toxicol. Appl. Pharmacol.* **172**, 62–74.

Foureman, P., Mason, J. M., Valencia, R., and Zimmering, S. (1994). Chemical mutagenesis testing in *Drosophila*: X. Results of 70 coded chemicals tested for the National Toxicology Program. *Environ. Mol. Mutagen* **23**, 208–227.

Ghissassi, F. E., Barbin, A., and Bartsch, H. (1998). Metabolic activation of vinyl chloride by rat liver microsomes: Low-dose kinetics and involvement of cytochrome P450 2E1. *Biochem. Pharmacol.* **55**, 1445–1452.

Guengerich, F. P. (1994). In *Analysis and Characterization of Enzymes in Principles and Methods of Toxicology*, 3rd ed. (A. Wallace Hayes, Ed.), pp. 1259–1313. Raven Press, New York.

Halpert, J. R., Guengerich, F. P., Bend, J. R., and Correia, M. A. (1994). Selective inhibitors of cytochromes P450. *Toxicol. Appl. Pharmacol.* **125**, 163–175.

Himmelstein, M. W., Acquavella, J. F., Recio, L., Medinsky, M. A., and Bond, J. A. (1997). Toxicology and epidemiology of 1,3-butadiene. *Crit. Rev. Toxicol.* **27**, 1–108.

Himmelstein, M. W., Carpenter, S. C., Evans, M. V., Kenyon, E. M., and Hinderliter, P. M. (2004). Kinetic modeling of β-chloroprene metabolism: II. The application of physiologically based modeling for cancer dose-response analysis. *Toxicol. Sci.* **79**, 28–37.

Himmelstein, M. W., Carpenter, S. C., Hinderliter, P. M., Snow, T. A., and Valentine, R. (2001a). The metabolism of β-chloroprene: Preliminary *in vitro* studies using liver microsomes. *Chem. Biol. Interact.* **135–136,** 267–284.

Himmelstein, M. W., Gladnick, N. L., Donner, E. M., Snyder, R. D., and Valentine, R. (2001b). *In vitro* genotoxicity testing of (1-chloroethenyl)oxirane, a metabolite of β-chloroprene. *Chem. Biol. Interact.* **135–136,** 703–713.

Jaeger, R. J., Connolly, R. B., Reynolds, E. S., and Murphy, S. D. (1975). Biochemical toxicology of unsaturated halogenated monomers. *Environ. Health Perspect.* **11,** 121–128.

Krause, R. J., Sharer, J. E., and Elfarra, A. A. (1997). Epoxide hydrolase-dependent metabolism of butadiene monoxide to 3-butene-1,2-diol in mouse, rat, and human liver. *Drug Metab. Dispos.* **25,** 1013–1015.

Kreuzer, P. E., Kessler, W., Welter, H. F., Baur, C., and Filser, J. G. (1991). Enzyme-specific kinetics of 1,2-epoxybutene-3 in microsomes and cytosol from livers of mouse, rat, and man. *Arch. Toxicol.* **65,** 59–67.

Lynch, J. (2001). Occupational exposure to butadiene, isoprene, and chloroprene . *Chem. Biol. Interact.* **135–136,** 147–154.

Lynch, M. A. (2001). Manufacture and use of chloroprene monomer. *Chem. Biol. Interact.* **135–136,** 155–167.

Malvoisin, E., Lhoest, G., Poncelet, F., Roberfroid, M., and Mercier, M. (1979). Identification and quantitation of 1,2-epoxy-3-butene as the primary metabolite of 1,3-butadiene. *J. Chromatogr.* **178,** 419–425.

Melnick, R. L., Elwell, M. R., Roycroft, J. H., Chou, B. J., Ragan, H. A., and Miller, R. A. (1996). Toxicity of inhaled chloroprene (2-chloro-1,3-butadiene) in F344 rats and B6C3F1 mice. *Toxicology* **108,** 79–91.

Melnick, R. L. and Sills, R. C. (2001). Comparative carcinogenicity of butadiene, isoprene, and chloroprene in rats and mice. *Chem.Biol. Interact.* **135–136,** 27–42.

Melnick, R. L., Sills, R. C., Portier, C. J., Roycroft, J. H., Chou, B. J., Grumbein, S. L., and Miller, R. A. (1999). Multiple organ carcinogenicity of inhaled chloroprene (2-chloro-1,3-butadiene) in F344/N rats and B6C3F1 mice and comparison of dose response with 1,3-butadiene in mice. *Carcinogenesis* **20,** 867–878.

Munter, T., Cottrell, L., Golding, B. T., and Watson, W. P. (2003). Detoxication pathways involving glutathione and epoxide hydrolase in the *in vitro* metabolism of chloroprene. *Chem. Res. Toxicol.* **16,** 1287–1297.

NTP (National Toxicology Program) (1998). *Toxicology and Carcinogenesis Studies of Chloroprene* (CAS No. 126–99–8) in F344/N Rats and B6C3F1 Mice (Inhalation Studies), Technical Report No. 467, NIH Publication No. 98–3957. National Institutes of Health, Bethesda, MD.

Plopper, C. G., Chang, A. M., Pang, A., and Buckpitt, A. R. (1991). Use of microdissected airways to define metabolism and cytotoxicity in murine bronchiolar epithelium. *Exp. Lung Res.* **17,** 197–212.

Plugge, H., and Jaeger, R. J. (1979). Acute inhalation toxicity of 2-chlorobutadiene (chloroprene): Effects on liver and lung. *Toxicol. Appl. Pharmacol.* **50,** 565–572.

Raham Q, Abidi, P., Afaq, F., Schiffmann, D., Mossman, B. T., Kamp, D. W., and Athar, M. (1999). Glutathione redox system in oxidative lung injury. *Crit. Rev. Toxicol.* **29,** 543–668.

Schmiedel, G., Filser, J. G., and Bolt, H. M. (1983). Rat liver microsomal transformation of ethene to oxirane *in vitro*. *Toxicol. Lett.* **19,** 293–297.

Seaton, M. J., Plopper, C. G., and Bond, J. A. (1996). 1,3-Butadiene metabolism by lung airways isolated from mice and rats. *Toxicology* **113,** 314–317.

Summer, K. H., and Greim, H. (1980). Detoxification of chloroprene (2-chloro-1,3-butadiene) with glutathione in the rat. *Biochem. Biophys. Res. Commun.* **96,** 566–573.

Tice, R. R. (1988). The cytogenetic evaluation of *in vivo* genotoxic and cytotoxic activity using rodent somatic cells. *Cell. Biol. Toxicol.* **4,** 475–486.

Tice, R. R., Boucher, R., Luke, A. A., Paquette, D. E., Melnick, R. L., and Shelby, M. D. (1988). Chloroprene and isoprene: Cytogenetic studies in mice. *Mutagenesis* **3,** 141–146.

Trochimowicz, H. J., Löser, E., Feron, V. J., Clary, J. J. and Valentine, R. (1998). Chronic inhalation toxicity and carcinogenicity studies on β-chloroprene in rats and hamsters. *Inhal. Toxicol.* **10,** 443–472.

Valentine, R., and Himmelstein, M. W. (2001). Overview of the acute, subchronic, reproductive, developmental, and genetic toxicology of β-chloroprene. *Chem. Biol. Interact.* **135–136,** 81–100.

Vogel, E. (1979). Mutagenicity of chloroprene, 1-chloro-1,3-trans-butadiene, 1,4-dichlorobutene-2, and 1,4-dichloro-2,3-epoxybutane in *Drosophila melanogaster. Mutat. Res.* **67,** 377–381.

Watson, W. P., Cottrell, L., Zhang, D., and Golding, B. T. (2001). Metabolism and molecular toxicology of isoprene. *Chem. Biol. Interact.* **135–136,** 223–238.

Zaridze, D., Bulbulyan, M., Changuina, O., Margaryan, A., and Boffeta, P. (2001). Cohort studies of chloroprene-exposed workers in Russia. *Chem. Biol. Interact.* **135–136,** 487–503.